Peer review status: This is a non-peer-reviewed preprint submitted to EarthArXiv.

The preprint was submitted to the Environmental Research Letters for peer review.

Authors *(affiliation and email)*:
Hikari Viviane Yamamoto Fukuda *(Department of Natural Environmental Studies, Graduate School of Frontier Sciences, The University of Tokyo, Kashiwa, Chiba, Japan; Institute of Industrial Science, The University of Tokyo, Kashiwa, Chiba, Japan; hikari.ldn@gmail.com)*,
Md. Rezuanul Islam *(Department of Civil Engineering, Graduate School of Engineering, The University of Tokyo, Bunkyo, Tokyo, Japan; fahim.islam@sogo.t.u-tokyo.ac.jp)*, and
Yohei Sawada *(Department of Civil Engineering, Graduate School of Engineering, The University of Tokyo, Bunkyo, Tokyo, Japan; yoheisawada@g.ecc.u-tokyo.ac.jp)*

Do Less Predictable Tropical Cyclones Induce Larger Damages?

Hikari Viviane Yamamoto Fukuda[1,2], Md. Rezuanul Islam[3], and Yohei Sawada[3]Hikari Viviane Yamamoto Fukuda[1,2]Md. Rezuanul Islam[3]Yohei Sawada[3]

[1]*Department of Natural Environmental Studies, Graduate School of Frontier Sciences, The University of Tokyo, Kashiwa, Chiba, Japan*
[2]*Institute of Industrial Science, The University of Tokyo, Kashiwa, Chiba, Japan*
[3]*Department of Civil Engineering, Graduate School of Engineering, The University of Tokyo, Bunkyo, Tokyo, Japan*
[*]*Corresponding author: hikari.ldn@gmail.com*
[1]*Department of Natural Environmental Studies, Graduate School of Frontier Sciences, The University of Tokyo, Kashiwa, Chiba, Japan*
[2]*Institute of Industrial Science, The University of Tokyo, Kashiwa, Chiba, Japan*
[3]*Department of Civil Engineering, Graduate School of Engineering, The University of Tokyo, Bunkyo, Tokyo, Japan*

Abstract

Tropical cyclones (TCs) cause substantial disaster losses worldwide. Forecast skill for TC track and intensity has been improved by enhanced observations, high-resolution numerical models, advanced data assimilation methods, and applications of machine-learning methods. Yet these improvements have not consistently translated into reduced losses, in part because disaster outcomes depend on many other elements, including communications between weather agency and the public. Therefore, it is not straightforward to observe the damage reduction by improved TC forecast, and the impact of the improvement of TC track and intensity forecast on damage has not been comprehensively quantified using real-world data. In this study, we examine 31 TCs that made landfall in Japan between 2006 and 2023 and quantify how errors in Joint Typhoon Warning Center (JTWC) operational TC track and intensity forecasts relate to flood-induced damage. To our knowledge, this is the first nationwide assessment for Japan linking operational TC forecast accuracy to observed TC-induced damages. Our multi-linear regression analysis reveals that along-track forecast error – distance between forecast and actual positions along the direction of travel – is positively associated with building and household damages ($p<0.05$), implying greater residential and structural impacts when forecasted TC positions deviate farther along the track. Conversely, landfall timing and intensity errors show no statistically significant association with flood damage. Despite the unclear causal relationships, these findings imply that further reductions in track error, particularly its along-track component, may contribute to mitigating TC-related flood losses.
Keywords: Tropical cyclones, forecast errors, flood damage, regression models, Japan

1 Introduction

Tropical cyclones (TCs) are among the most costly weather-related hazards (Wirtz et al., 2014), resulting in significant human and economic losses across many regions (Ito, 2016; Roy & Kovordányi, 2012). Over the past fifty years, TCs have caused more than 700,000 deaths (World Meteorological Organization, 2020). An estimated 18 % of the global population lives in vulnerable TC-prone

areas, and more than 25 % of the global GDP is at considerable risk (Dilley, 2005). TCs also present substantial risks to infrastructure and the livelihoods, especially in coastal areas and island countries (Hanson et al., 2011; Peduzzi et al., 2012). Impactful TCs can strike across diverse locations, affecting both major economic centers and smaller regions (Islam & Sawada, 2025). In Japan, for example, TC Hagibis (2019) – one of the most severe events in recent decades (Islam & Sawada, 2025; Shimozono et al., 2020) – resulted in riverbank breaches at 135 points across 71 rivers, cut power to 270,000 homes, claimed at least 86 lives, and caused an estimated USD 400 billion in economic damage (LeComte, 2020).

To address TC impacts, meteorologists have worked for decades to enhance forecasts of track (Ito, 2016), intensity (Shi & Xu, 2024), landfall timing (Leroux et al., 2018) and rainfall (Ren et al., 2007). Forecasts are commonly evaluated using metrics such as haversine position error, along-track error, intensity error, landfall time error, and landfall position error. Advances in satellite observing systems, numerical weather prediction, and ensemble methods have reduced forecast errors and extended lead times for early warnings (Ito, 2016; McAdie & Lawrence, 2000), especially in developed countries (Ito, 2016). For instance, improvements in forecast landfall position (31-54 h lead) and landfall time (19-30 h lead) errors in the United States (US) from 1975 to 2000 were observed, with decreases of ∼35 km and ∼1.5 h, respectively (Powell & Aberson, 2001). Ito (2016) reported that in Japan, the mean 24-h track forecast position error decreased from ∼210 km in the 1980s to ∼90 km by 2014 — an improvement of over 50 % — consistent with Atlantic Basin trends (Cangialosi et al., 2020). Early warning systems have also evolved significantly: 72-h forecasts became operational before 2000, with 96-h and 120-h forecasts introduced around 2010 in Japan (Ito, 2016). While Ito (2016) noted an increasing trend in intensity forecast errors during 1992-2014, potentially linked to the increase of stronger TCs, after employing statistical corrections, the TC intensity forecast was significantly improved by 7.8-16.9 %. Other studies suggest that this previous increasing trend of intensity error is changing. For example, in the Atlantic Basin, Cangialosi et al. (2020) found that intensity forecast errors declined by ∼6 kt between 2000–2009 and 2010–2019 at 72-120 h, and by ∼2 kt at 24-h forecast. More recently, Minamide and Posselt (2025) reported major improvements from assimilating all-sky infrared satellite radiances, reducing early-stage negative bias and lowering peak intensity errors by ∼20 % relative to concurrent operational guidance.

Despite substantial progress, the extent to which improved TC forecasts reduce disaster impacts remains insufficiently quantified. In principle, higher accuracy and longer lead times should enable better decisions and mitigate losses (Barrett et al., 2006; Martinez, 2020; Roy & Kovordányi, 2012), but direct empirical links to socioeconomic or physical damages are limited. For instance, reduced forecast errors during Hurricane Ivan (2004) were estimated to save lives and avoid billions in damages and unnecessary evacuation costs in the US (Barrett et al., 2006). More recently, Salomon (2024) quantified the economic value of improved hurricane forecasts in the US by integrating storm-track and intensity predictions with county-level expenditure and damage data. Their findings indicated that forecast accuracy gains between 2007 and 2020 yielded an average reduction of $5 billion per hurricane (∼19 % of total losses). While this study offers valuable quantitative insights into the financial benefits of enhanced wind-speed forecasts, it primarily addresses pre-landfall protective spending and post-landfall recovery expenditures.

A further limitation in assessing the socio-economic effects of forecast improvements is data availability. Long-term consistent databases that jointly include meteorological, hazard, and impact information remain scarce (Knapp et al., 2010; Meiler et al., 2022). When such data exist, they are often difficult to access or not organized for research, hindering comparative and cross-regional assessments (Islam & Sawada, 2025). Consequently, it is unclear whether forecast advances have produced tangible reductions in physical damages or improved preparedness outcomes, particularly where observational and impact datasets are limited. Addressing this knowledge gap is essential for integrating forecast skill improvements into disaster risk reduction and policy.

To address this research gap, we examine the relationship between forecast errors and reported flood-related damages from TCs in Japan. Specifically, we analyze along-track error, as well as errors in wind intensity, landfall timing, and landfall locations, and their statistical associations with human and economic losses. This study focuses on TCs that made landfall in Japan between 2006 and 2023, a period with consistent availability of high-quality forecast and damage data. Within this timeframe, 31 landfalling TCs were identified and analyzed. Japan was selected as the

study area due to the accessibility of comprehensive observational and impact datasets (Kato & Tajima, 2023; Takagi et al., 2023), including the Digital Typhoon Database by Digital Typhoon (2025a), and a well-established forecasting and disaster reporting infrastructure. By quantifying these relationships, this study aims to clarify how forecast accuracy influences societal outcomes and to inform improvements in early warning and risk communication strategies.

2 Data and Methods

2.1 Analyzed TC

Multiple datasets were used to analyze relationships between TC forecast errors and flood damages in Japan. The datasets include best track and forecast data to assess the impact of forecast accuracy on socio-economic and damage statistics. From the Digital Typhoon website (Digital Typhoon, 2025b), we identified all TCs that made landfall in the main islands of Japan (Hokkaido, Honshu, Kyushu, and Shikoku) between 2006 and 2023. Thus, it excluded passage TCs (when the center of the TC crosses a small island or peninsula and then returns to the sea in a short period of time). The analysis period covers 2006 to 2023, ensuring consistency with the available forecast and damage records. Finally, to ensure sufficient temporal and spatial data coverage for evaluating forecast performance, we applied a lifecycle-based TC selection criterion: only landfalling TCs that persisted for at least five days prior to landfall in both forecast and observational records were included. This threshold excludes short-lived or weak systems whose limited track data could lead to unreliable error estimates. Applying these criteria resulted in 31 TCs selected for analysis.

2.1.1 Best track and wind intensity data

Best track positions and wind intensity for the selected TCs were obtained from the Joint Typhoon Warning Center (2025) (JTWC), which provides post-analysis TC center positions, 1-minute sustained wind speeds, and minimum central pressures at 6-hour intervals. JTWC, operated by the United States Navy and Air Force, issues TC forecasts over the Western Pacific and other ocean basins. Best track positions and intensities are produced from a retrospective reanalysis intended to best represent actual conditions. Analysts integrate geostationary and polar-orbiting satellite imagery, microwave data, scatterometer winds, and observational reports. For intensity estimate, JTWC primarily relies on the Dvorak Technique, which interprets cloud patterns in visible and infrared imagery to assign a T-number that corresponds to a wind intensity. Additional data and observational reports are incorporated to refine the final intensity. This best track dataset served as the verification ("truth") for computing forecast errors, including along-track error, great circle (haversine) position error, wind speed intensity error, and landfall time error.

2.1.2 Forecast data

Operational JTWC forecasts for all 31 landfalling TCs were sourced from the Regional and Mesoscale Meteorology Branch (2025) (RAMMB) of NOAA/NESDIS. For each advisory, typically issued every 6-h, the dataset provides the analyzed (0-h) position/intensity and forecast track positions and 1-minute sustained winds at 12-h, 24-h, 36-h, 48-h, 72-h, 96-h, and 120-h lead times. These official advisories are real-time estimates and are not retrospectively reanalyzed; hence, they differ from best track data. JTWC supplies Western North Pacific digital forecast data to RAMMB through databases in the Automated Tropical Cyclone Forecast (ATCF) system (Sampson & Schrader, 2000). Forecast errors were computed for each TC and lead time by verification against JTWC best track information.

Although Japanese residents primarily receive TC forecasts from the Japan Meteorological Agency (JMA), the use of JTWC data is justified for three reasons. First, the RAMMB archive (i.e., JTWC operational forecasts) offers a consistent, publicly accessible record of official TC forecasts from 2006 to the present, enabling systematic computation of forecast errors for all landfalling TCs. On the other hand, JMA forecast data is not publicly accessible. Second, JTWC forecasts are consensus products that combine multiple global deterministic models and ensemble means (e.g., European Centre for Medium-Range Weather Forecasts (ECMWF), United Kingdom Met

Office (UKMO), US Navy Global Environmental Model (NAVGEM), JMA Global Spectral Model). Similarly, JMA's operational track forecasts are consensus products, integrating forecasts from JMA, ECMWF, UKMO, and the National Centers for Environmental Prediction (NCEP). Third, previous studies, such as Conroy et al. (2023), suggest that JTWC forecast track errors are often comparable to NCEP-based guidance, which contributes to the JMA consensus. Furthermore, Huang et al. (2021) showed that JTWC intensity forecast error is strongly correlated with JMA forecast error. Therefore, although the exact forecasts communicated to Japanese society may differ, JTWC forecast errors serve as a reasonable proxy for evaluating potential societal impacts of uncertainty in TC forecast.

2.1.3 Damage and socioeconomic data

Economic loss statistics and damage reports for each landfalling TC were compiled from two complementary sources: e-Stat (2025), Japan's official statistical portal managed by the Statistics Bureau of Japan, and the Digital Typhoon (2025a) database developed by the National Institute of Informatics (NII). The e-Stat platform provides verified governmental records, including monetary estimates of direct and indirect disaster losses, while Digital Typhoon offers event-based summaries of fatalities, injuries, damaged or destroyed houses, inundated buildings, and estimated economic losses derived from disaster reports and governmental bulletins.

For each TC, impact variables were extracted to represent human, structural, and economic losses, including total economic losses, number of fatalities, injuries, affected households and employees, and the number of houses damaged, destroyed, or inundated. Cross-validation was performed by comparing corresponding entries across the two databases and with local disaster reports and the dataset by Sawada et al. (2025), to identify inconsistencies, missing values, or reporting biases. When discrepancies occurred (e.g., in total loss estimates or casualty counts), priority was given to the official e-Stat values, while Digital Typhoon was used to supplement information unavailable in e-Stat.

Other damage and socioeconomic variables, such as flooded area (m^2), total municipal area (km^2), total population (persons), population density (persons m^{-2}), and income per capita (JPY person^1), were compiled from e-Stat and local reports at the municipal level to capture spatial variations in exposure and vulnerability.

Municipal-level socioeconomic variables were aggregated for each TC to construct a single event-level record that matched the temporal and spatial coverage of the forecast and best-track datasets. To ensure comparability across events and years, all monetary values were converted to Japanese yen (JPY) and adjusted to 2022 real values using the Consumer Price Index (CPI) published by the Statistics Bureau of Japan. This standardization enabled consistent assessment of the relationship between forecast performance and socioeconomic impacts.

2.1.4 Data integration and matching

Each TC case was matched across the three datasets (Table 1) — the JTWC best tracks, JTWC forecasts, and impact statistics from e-Stat and Digital Typhoon — using event name, year, and landfall date as matching criteria. Forecast and best-track datasets were temporally synchronized to calculate the forecast error metrics, including along-track error (ATE), haversine position error, landfall time error (LTE), and wind intensity error at each lead time.

To estimate total damage for each landfalling TC, reported damages were first identified by matching the reported period and TC number in e-Stat with the corresponding storm in the JTWC record. All direct damages (e.g., infrastructure, agriculture, housing, and public facilities) attributed to the same TC were then aggregated to form a single total loss value per event. When inconsistencies or missing values were found, the dataset was supplemented with prefectural or municipal disaster reports to ensure completeness.

Finally, each TC case was summarized as a unified record integrating forecast accuracy metrics with corresponding human and economic losses. This harmonized dataset of 31 landfalling TCs (2006-2023) provides a novel and consistent foundation for quantitatively examining the relationships between forecast skill and societal impacts in Japan.

Table 1: Summary of the factors used in this study.

Category	Variable	Description	Source
Forecast Data	Forecast track (lat, lon)	6-hourly forecasted TC center positions up to 120 h	JTWC / RAMMB
	Forecast intensity	1-min sustained wind speed (knots) for each forecast advisory	
Observed Data	Best-track position and intensities	Post-event verified TC center positions and intensities	JTWC Best Track
Forecast Error	Along-Track Error (ATE)	Distance (km) between forecast and best-track positions along the storm motion vector	Computed from forecast, and observations
	Haversine position error	Great-circle distance (km) between predicted and actual position	
	Landfall Time Error (LTE)	Difference (hours) between forecasted and observed landfall time	
	Intensity error	Difference between predicted and actual wind intensity speeds	
Impact Data	Fatalities	Number of reported deaths caused by TC	e-Stat, Digital Typhoon, Prefectural reports
	Injuries	Number of reported injuries	
	Affected households	Number of affected households	
	Affected employees	Number of affected employees	
	Buildings flooded	Number of flooded buildings above and under floor	
	Buildings destroyed	Number of completely destroyed residential buildings	
	Buildings damaged	Number of partially damaged residential buildings	
	Economic losses	Estimated total economic losses (JPY, adjusted to 2022)	

2.2 Methodology

2.2.1 Calculation of forecast errors

Forecast accuracy was assessed by comparing the JTWC best track positions, intensities, and landfalling time with the JTWC forecasts at multiple lead times (0, 12, 24, 36, 48, 72, 96 and 120 hours). The following error metrics were computed:

(1) Position error (PE, km). The position error measures the great-circle distance between the forecasted and observed cyclone centers, accounting for Earth's curvature. It was calculated using the haversine formula:

$$\mathrm{PE} = 2R \arcsin\left(\sqrt{\sin^2\left(\frac{\phi_\mathrm{f} - \phi_\mathrm{obs}}{2}\right) + \cos(\phi_\mathrm{obs})\cos(\phi_\mathrm{f})\sin^2\left(\frac{\lambda_\mathrm{f} - \lambda_\mathrm{obs}}{2}\right)}\right), \tag{1}$$

where R is Earth's equatorial radius (6,378 km), and (ϕ, λ) are latitude and longitude for the forecast (f) and observed (obs) TC positions.

(2) Along-track error (ATE, km). The along-track error represents the displacement of the forecasted TC position in the direction of its motion relative to the observed (best-track) position.

The ATE was calculated as the projection of the forecast position error vector onto the observed direction of motion:

$$\mathrm{ATE} = \Delta\mathbf{r} \cdot \hat{\mathbf{t}}_{\mathrm{obs}} = |\Delta\mathbf{r}| \cos(\theta) = \mathrm{PE}\cos(\theta), \tag{2}$$

where $\Delta\mathbf{r}$ is the vector difference between forecast ($\mathbf{r}_{\mathrm{f}}$) and best-track ($\mathbf{r}_{\mathrm{obs}}$) positions, and $\hat{\mathbf{t}}_{\mathrm{obs}}$ is the unit tangent vector along the observed track direction between consecutive best-track points.

(3) Landfall time error (LTE, h). The landfall time error quantifies the timing discrepancy between the forecasted landfall time and the observed landfall time obtained from the Digital Typhoon database:

$$\mathrm{LTE} = t_{\mathrm{f}}^{L} - t_{\mathrm{obs}}^{L}, \tag{3}$$

where t_{f}^{L} is the forecasted landfall time, and t_{obs}^{L} is the reported landfall time in Digital Typhoon. The landfall time was defined as the forecast advisory hour at which the TC center first crossed the Japanese coastline. Because advisories are issued every 6 hours, we assigned landfall using the nearest forecast advisory time, without temporal interpolation, to ensure consistency with the official forecast schedule. A positive LTE indicates the forecast landfall occurs later than observed. Since the JTWC best-track dataset does not explicitly provide landfall time information, the actual landfall time (t_{obs}^{L}) was obtained from the Digital Typhoon Database, which reports the time when the TC center crosses the Japanese coastline.

(4) Wind intensity error (WIE, kt). The wind intensity error represents the difference between forecasted and observed 1-minute sustained maximum 10-m wind speeds:

$$\mathrm{WIE} = V_{\mathrm{f}} - V_{\mathrm{obs}}, \tag{4}$$

where V_{f} and V_{obs} denote the forecasted and best-track maximum wind intensities, respectively.

Each forecast case was evaluated at multiple lead times, and the errors were summarized by event to assess overall forecast skill and its relation to observed human and economic impacts.

2.2.2 Regression model construction

To investigate how forecast accuracy relates to damage indicators, multiple linear regression models were developed based on the structure proposed by Sawada et al. (2025). The general form of the model is given by a multi-linear regression equation:

$$Y = \beta_0 + \sum_{i=1}^{n} \beta_i X_i \tag{5}$$

where Y represents the flood-related damages (dependent variable), and X_1-X_n to represent the explanatory variables.

Because TCs generate a wide range of impacts, the analysis does not rely on a single definition of "damage." Instead, thirteen dependent variables (Y) were examined, capturing physical, economic, agricultural, and human impacts, for which simple introduction is made in Table 1. Modeling each Y separately allows for the assessment of whether forecast errors influence different types of losses in different ways. The dependent variables were

- Y_1: Flooding above floor (number of buildings),
- Y_2: Flooding above flood (50-99 cm, number of buildings),
- Y_3: Flooding above flood (1-49 cm, number of buildings),
- Y_4: Flooding under floor (number of buildings),
- Y_5: Completely destroyed/washed away buildings (number of buildings),

- Y_6: Partially destroyed buildings (number of buildings),
- Y_7: Total buildings affected (number of buildings),
- Y_8: Injured persons (persons),
- Y_9: Dead or missing persons (persons),
- Y_{10}: Affected employees (persons),
- Y_{11}: Affected farming/fishing households,
- Y_{12}: Affected residential households,
- Y_{13}: General asset damage (thousand JPY).

The explanatory variables used in this study were:

- Forecast error metrics (ATE, position, landfall time, and intensity error),
- Flooded area (m^2),
- Total area of the affected municipalities (km^2),
- Total population of the affected municipalities (persons),
- Population density (persons km^{-2}),
- Income per capita (JPY $person^{-1}$), and
- TC year.

Y and all explanatory variables except for the total area of affected municipalities, population density, income per capita, and TC year were log-transformed to normalize their distributions and to allow for comparability of coefficients across variables. Before the regression analysis, forecast errors were transformed to absolute values, and zero values in variables were substituted with one. This transformation also mitigates the influence of extreme values, ensuring a more stable estimation of the regression parameters.

2.2.3 Statistical tests and model evaluation

Statistical significance of the regression coefficients was assessed using p-values (threshold $p < 0.05$) and 95 % confidence intervals. To ensure model reliability, multicollinearity was checked using the variance inflation factor (VIF), and normality of residuals were verified with plots of the residuals with the fitted and Q-Q plots. Model fit was evaluated with the coefficient of determination (R^2) and adjusted R^2, while consistency across years was examined through cross-validation and comparison with observed loss patterns.

3 Results

The regression models indicate that forecast-skill metrics explain a substantial portion of the variability in damages associated with the 31 landfalling TCs. Across all specifications, ATE is the only forecast-error metric that shows statistically significant positive associations with multiple building-and household-related flood impacts (Fig. 2d). In contrast, landfall time error, wind intensity error, and haversine position error are not statistically significant at the 5 % level (Figs. 2a–c). Across the 52 model specifications (13 damage outcomes x 4 forecast-error metrics), model performance is consistently high, with R^2 ranging from 0.5 to 0.93 and adjusted R^2 from 0.35 to 0.91 (Table 2). RMSE values range from 0.5 to 1.29 (Table 2). Overall model F-tests are statistically significant for all specifications ($p < 0.05$; Table 2), indicating that predictors are jointly associated with the outcomes. Because model performance is evaluated on the same dataset used for estimation, these statistics reflect in-sample explanatory power.

Fig. 1 presents observed versus fitted log-transformed general assets damages for the model using ATE as the forecast-skill predictor. The fitted values closely follow the 1:1 reference line, with R^2 =0.839 and adjusted R^2 =0.790 (RMSE of 0.93; overall model F-test p-value = 9.55810^{-8}; Fig. 1). Figure 1 also shows that model skill is maintained across most of the damage range, with only a small number of events showing larger residuals relative to the 1:1 line. VIF diagnostics indicate substantial multicollinearity among several covariates (Table 1). In particular, total population and TC year exhibit very large VIF values across many specifications, with total flooded area also consistently elevated. In contrast, population density and total area show comparatively lower VIF values (Table 3). Notably, the forecast-error terms themselves differ markedly in collinearity: intensity and landfall-time errors show consistently low VIF values (typically <10), whereas the track-displacement terms — especially haversine error and, to a lesser extent, along-track error — exhibit substantially larger VIF values across outcomes (Table 1). Given this multicollinearity, coefficients for highly correlated covariates should be interpreted cautiously. Therefore, we focus on sign and significance patterns that are consistent across model specifications.

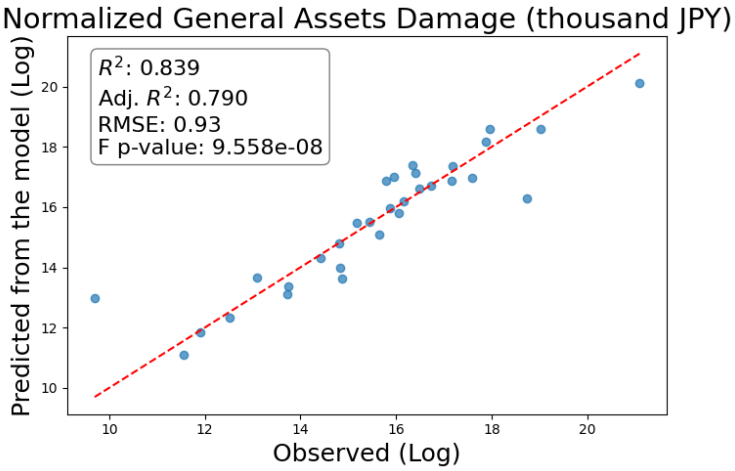

Figure 1: Observed versus fitted values of log-transformed general asset damage (thousand JPY) from the multilinear regression model using along-track forecast error as the forecast-skill predictor. Blue markers represent landfalling TC event selected in this study (n=31). The dashed line indicates the 1:1 reference.

Figure 2 compares estimated coefficients for the forecast-error term across outcomes and error metrics. Landfall-time error and intensity error show highly similar sign patterns across outcomes (9 of 13 coefficients share the same sign for each metric), but none of the coefficients are statistically significant at $p < 0.05$ (Fig. 2a-b). Haversine position error and ATE also show broadly similar sign patterns (10 of 13 coefficients share the same sign; Figs. 2c–d). However, only ATE yields statistically significant positive coefficients (95 % confidence interval: error bars do not cross zero) for five outcomes: flooding above floor (total), flooding above floor (1–49 cm), flooding under floor, affected households (under floor), and total buildings affected (Fig. 2d). It suggests that ATE-damage linkage is strongest for prevalent inundation-and impacted household-count outcomes rather than human impacts (i.e., injured, dead or missing) captured in the dataset. By contrast, coefficients for the remaining forecast-error metrics (Figs. 2a–c) do not reach statistical significance, and their effect sizes are generally smaller.

Table 2: Summary of the performance of the regression models.

Damage type	Error metric	R^2	Adjusted R^2	RMSE	F p-value
General assets	Haversine error	0.833	0.782	0.95	1.47E-07
	ATE	0.839	0.790	0.93	9.56E-08
	Intensity error	0.829	0.776	0.96	1.94E-07
	Landfall time error	0.837	0.787	0.94	1.12E-07
Flooding above floor (Total)	Haversine error	0.919	0.895	0.62	4.27E-11
	ATE	0.928	0.906	0.59	1.12E-11
	Intensity error	0.902	0.873	0.69	3.68E-10
	Landfall time error	0.914	0.888	0.64	8.42E-11
Flooding above floor (50-99 cm)	Haversine error	0.901	0.871	0.65	4.34E-10
	ATE	0.901	0.871	0.65	4.27E-10
	Intensity error	0.874	0.836	0.74	6.31E-09
	Landfall time error	0.904	0.874	0.64	3.16E-10
Flooding above floor (1-49 cm)	Haversine error	0.914	0.888	0.62	8.68E-11
	ATE	0.924	0.901	0.59	2.10E-11
	Intensity error	0.885	0.850	0.72	2.22E-09
	Landfall time error	0.908	0.880	0.65	1.88E-10
Flooding under floor	Haversine error	0.849	0.803	0.74	4.82E-08
	ATE	0.876	0.839	0.67	5.16E-09
	Intensity error	0.789	0.725	0.88	1.90E-06
	Landfall time error	0.842	0.794	0.76	7.86E-08
Completely destroyed/washed away	Haversine error	0.785	0.719	0.88	2.38E-06
	ATE	0.776	0.707	0.90	3.68E-06
	Intensity error	0.723	0.638	1.00	3.60E-05
	Landfall time error	0.775	0.707	0.90	3.80E-06
Partially destroyed buildings	Haversine error	0.777	0.709	1.17	3.47E-06
	ATE	0.757	0.682	1.23	8.96E-06
	Intensity error	0.733	0.652	1.28	3.40E-05
	Landfall time error	0.731	0.649	1.29	2.58E-05
Injured	Haversine error	0.628	0.515	0.82	7.73E-04
	ATE	0.605	0.485	0.85	1.43E-03
	Intensity error	0.500	0.348	0.95	1.43E-02
	Landfall time error	0.594	0.471	0.86	1.88E-03
Dead or missing	Haversine error	0.788	0.724	0.50	1.97E-07
	ATE	0.767	0.696	0.52	5.52E-06
	Intensity error	0.771	0.701	0.52	4.59E-06
	Landfall time error	0.782	0.715	0.51	2.73E-06
Affected employees	Haversine error	0.854	0.810	0.89	3.25E-08
	ATE	0.850	0.804	0.90	4.42E-08
	Intensity error	0.709	0.621	1.26	5.92E-05
	Landfall time error	0.856	0.813	0.88	2.76E-08
Affected farming/fishing households	Haversine error	0.903	0.874	0.59	3.25E-10
	ATE	0.917	0.891	0.55	6.17E-11
	Intensity error	0.821	0.767	0.80	3.08E-07
	Landfall time error	0.904	0.875	0.59	2.94E-10
Affected households (under floor)	Haversine error	0.829	0.776	0.82	1.95E-07
	ATE	0.857	0.814	0.75	2.60E-08
	Intensity error	0.754	0.679	0.98	1.02E-05
	Landfall time error	0.820	0.765	0.84	3.37E-07
Total buildings affected	Haversine error	0.854	0.810	0.76	3.28E-08
	ATE	0.874	0.835	0.71	6.61E-09
	Intensity error	0.815	0.758	0.85	4.59E-07
	Landfall time error	0.852	0.807	0.76	3.80E-08

Table 3: VIF for each regression models' variables.

Damage type	Error metric	Error	Total flooded area	Total area	Total population	Population density	Income per person	TC year
General assets	Haversine	195.5	188.0	9.2	410.5	3.1	56.2	357.9
	ATE	40.6	193.7	9.2	409.3	3.1	60.1	253.7
	Intensity	8.7	183.8	9.2	382.7	3.2	53.0	210.1
	Landfall time	7.7	216.3	9.2	536.8	3.2	56.3	236.8
Flooding above floor (Total)	Haversine	195.5	188.0	9.2	410.5	3.1	56.2	357.9
	ATE	40.6	193.7	9.2	409.3	3.1	60.1	253.7
	Intensity	8.7	183.8	9.2	382.7	3.2	53.0	210.1
	Landfall time	7.7	216.3	9.2	536.8	3.2	56.3	236.8
Flooding above floor (50-99 cm)	Haversine	156.0	241.9	13.0	1030.0	3.5	56.1	666.5
	ATE	44.8	244.2	12.6	935.5	3.5	64.8	689.9
	Intensity	9.4	251.1	11.6	723.6	3.5	53.4	524.7
	Landfall time	7.4	282.4	12.5	1010.8	3.5	56.9	661.0
Flooding above floor (1-49 cm)	Haversine	195.5	188.0	9.2	410.5	3.1	56.2	357.9
	ATE	40.6	193.7	9.2	409.3	3.1	60.1	253.7
	Intensity	8.7	183.8	9.2	382.7	3.2	53.0	210.1
	Landfall time	7.7	216.3	9.2	536.8	3.2	56.3	236.8
Flooding under floor	Haversine	195.5	188.0	9.2	410.5	3.1	56.2	357.9
	ATE	40.6	193.7	9.2	409.3	3.1	60.1	253.7
	Intensity	8.7	183.8	9.2	382.7	3.2	53.0	210.1
	Landfall time	7.7	216.3	9.2	536.8	3.2	56.3	236.8
Completely destroyed/washed away floor	Haversine	151.2	327.5	17.3	1709.4	15.0	87.0	1014.4
	ATE	39.4	326.9	14.2	1155.9	13.0	83.5	872.9
	Intensity	9.4	368.1	13.2	1188.7	13.7	82.2	785.6
	Landfall time	6.3	358.0	13.8	1146.4	13.0	84.3	831.2
Partially destroyed buildings	Haversine	155.0	209.5	8.7	455.9	3.0	60.8	290.8
	ATE	42.0	214.0	8.8	439.0	3.0	66.8	230.8
	Intensity	7.7	202.2	8.9	425.0	3.2	61.1	186.0
	Landfall time	7.2	241.4	8.9	621.6	3.2	67.3	214.5
Injured	Haversine	198.7	189.3	9.1	396.4	3.1	53.6	353.8
	ATE	50.2	202.3	9.5	393.7	3.1	58.2	256.9
	Intensity	8.5	181.0	8.7	365.5	3.2	52.0	202.8
	Landfall time	7.9	219.6	8.7	524.6	3.2	56.7	229.0
Dead or missing	Haversine	167.7	250.2	12.3	821.5	3.3	76.0	528.1
	ATE	49.6	255.9	11.8	721.1	3.2	82.5	551.3
	Intensity	8.3	253.5	11.6	573.2	3.3	78.3	471.3
	Landfall time	7.1	289.0	11.8	639.3	3.2	76.2	513.8
Affected employees	Haversine	197.4	184.2	11.5	831.8	3.5	63.7	591.4
	ATE	45.4	190.7	11.4	826.4	3.5	70.9	599.2
	Intensity	8.9	180.7	10.9	652.2	3.6	58.5	487.6
	Landfall time	7.8	213.8	11.4	803.8	3.5	61.6	589.8
Affected farming/ fishing households	Haversine	194.8	333.2	20.4	2470.6	16.4	89.2	1501.2
	ATE	43.5	333.2	15.1	1417.6	13.6	83.2	1120.2
	Intensity	9.8	381.3	13.2	1217.2	15.0	82.0	858.7
	Landfall time	6.5	362.4	14.4	1331.9	13.7	85.2	1000.4
Affected households (under floor)	Haversine	195.5	188.0	9.2	410.5	3.1	56.2	357.9
	ATE	40.6	193.7	9.2	409.3	3.1	60.1	253.7
	Intensity	8.7	183.8	9.2	382.7	3.2	53.0	210.1
	Landfall time	7.7	216.3	9.2	536.8	3.2	56.3	236.8
Total buildings affected	Haversine	195.5	188.0	9.2	410.5	3.1	56.2	357.9
	ATE	40.6	193.7	9.2	409.3	3.1	60.1	253.7
	Intensity	19.6	273.6	12.8	956.4	4.6	48.2	708.3
	Landfall time	7.7	216.3	9.2	536.8	3.2	56.3	236.8

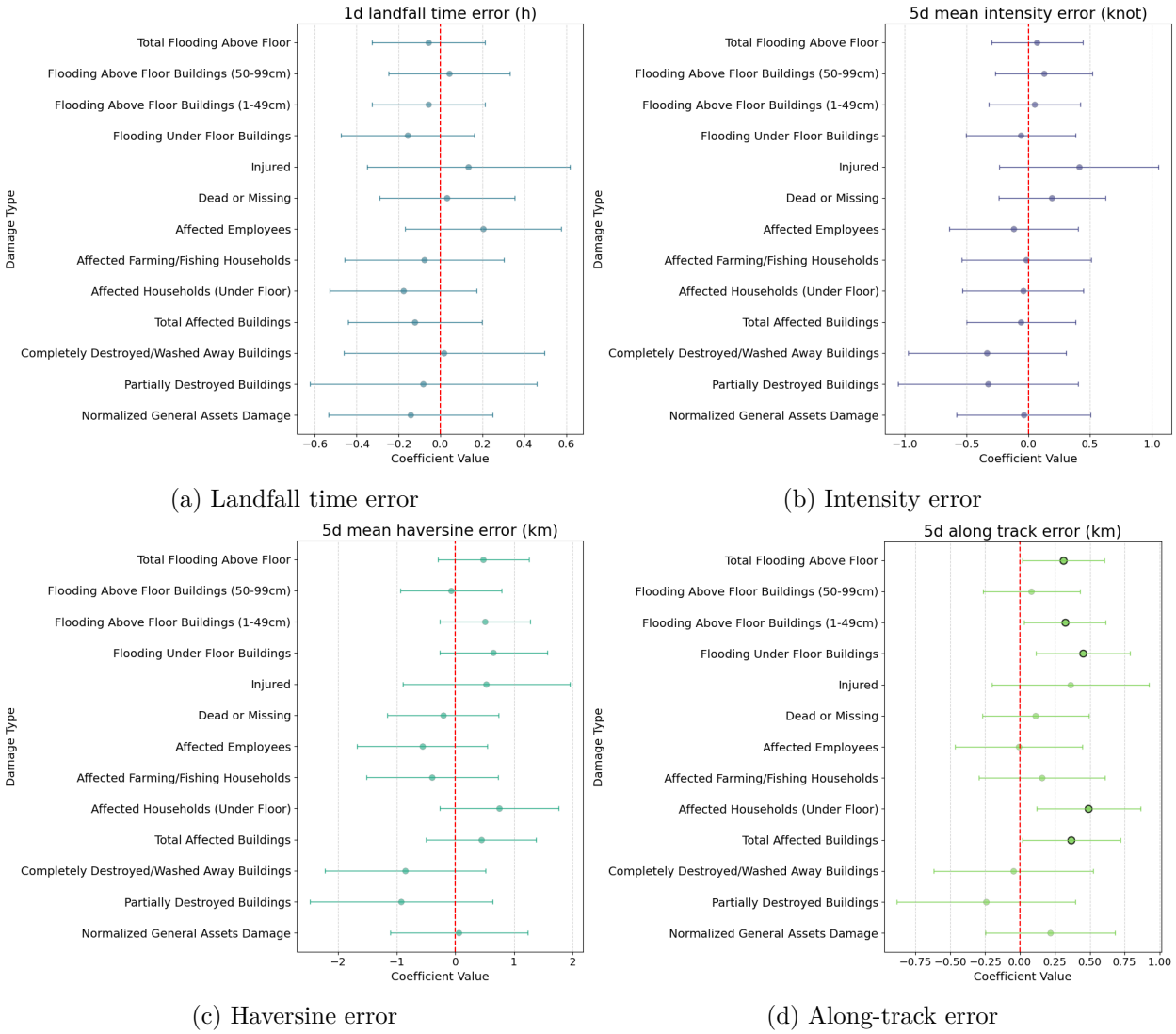

(a) Landfall time error

(b) Intensity error

(c) Haversine error

(d) Along-track error

Figure 2: Estimated regression coefficients for forecast error term across models for different damage/impact indicators: (a) landfall time error, (b) intensity error, (c) haversine track error, and (d) along-track error (ATE). Coefficients are computed using errors summarized over 5 days prior to landfall (except landfall-time error: 1 day prior). Points denote coefficient estimates; error bars represent 95 % confidence intervals; points with black-colored outline indicate $p < 0.05$.

Figure 3 summarizes the relationships between the control variables (socioeconomic and exposure related factors) and the thirteen damage outcomes across the four forecast error specifications. Cells report coefficient sign consistency and a consistency count (1–4), defined as the number of specifications in which the coefficient is statistically significant (p <0.05). Total flooded area shows the most consistent association with impacts, with positive and statistically significant coefficients for most damage outcomes (often significant in all four specifications; Fig. 3). It suggests that municipalities with larger flood-affected areas tend to experience higher losses across several categories (e.g., buildings affected, household flooding, residential damage). Other variables show significant associations in some cases, but their patterns are comparatively less stable. For example, taxable income per person is consistently negative and statistically significant for several building-flooding indicators, including above-floor flooding (1–49 cm and 50–99 cm) and under-floor flooding (Fig. 3). It indicates that wealthier municipalities tend to have more resilient structures or better flood protection measures. Population density shows two robust but opposing patterns: it is negatively associated with affected farming/fishing households and positively associated with above-floor flooding (50–99 cm; Fig. 3). This pattern is likely consistent with an urban-rural contrast. Total area is positively and consistently significant for above-floor flooding (50–99 cm) and partially destroyed buildings, while total population is positively associated with affected employees (Fig. 3). Importantly, some damage indicators — such as the number of injuries — show limited

significant association with any of the exposure variables, including flooded areas. The relatively good regression accuracy for impact indicators suggests that these outcomes are strongly shaped by structural and exposure-related factors represented in our dataset. Injury outcomes, however, are typically more sensitive to event-specific and behavioral factors (e.g., preparedness, emergency response), leading to larger unexplained variability. Thus, the lower accuracy for injury prediction reflects the greater influence of situational factors on human impacts, rather than a weakness of our modeling approach. Finally, some temporal patterns are also noticeable from Fig. 3. For example, TC year shows a positive association with impacts on farming and fishing households — suggesting a growing exposure or vulnerability in this sector — while showing a declining association with under-floor household impacts.

Figure 3: Sign and consistency of statistically significant control-variable coefficients across regression models. Shading indicates coefficient sign (positive in red, negative in blue, or mixed signs in pink) and number within each cell represent the consistency count, defined as the number of models (out of four, corresponding to landfall-time, intensity, haversine, and along-track errors) in which the coefficient is statistically significant ($p < 0.05$)

4 Conclusions and discussions

TC forecasts and their errors are fundamental to improving decision-making and minimizing damage impacts. Although the relationship between forecast quality and damages seems intuitive, for example, larger forecast errors can hinder appropriate preparation and increase damages, it has not been directly evaluated in previous research. Addressing this gap statistically, our findings show that along-track error is positively correlated with damages, especially building-related damages (e.g., number of underfloor and above floor [1-49 cm] flooded buildings, total affected structures). Such effects are more evident for buildings than for human impacts because buildings are immobile and directly exposed to wind and water (Kaźmierczak & Cavan, 2011). As a result, structural damage tends to scale more predictably with hazard intensity and track proximity. Moreover, when the expected path is forecasted incorrectly or not clearly understood by residents and local authorities, timely actions to protect buildings (e.g., sandbagging, securing windows, and relocating valuables) may not occur. Because buildings cannot be moved out of harm's way, insufficient or delayed preparedness leads to greater and more easily observable physical damage (Morss et al., 2010). The stronger performance of along-track error likely reflects its ability to capture timing

displacement — whether the cyclone was predicted to be ahead of or behind its actual position (Leonardo & Colle, 2020). This distinction is operationally important because earlier- or later-than-expected arrival directly influences when preparedness measures (e.g., shuttering, port closures, and evacuation) are initiated in the areas that ultimately experience peak impacts. In this sense, along-track error links more closely to the timing and spatial placement of protective actions than haversine position error, which conflates spatial deviations without indicating whether the cyclone arrived sooner or later. Compared with intensity and landfall-time errors — which are more variable and less consistently related to local impacts — the along-track error component exhibited a more stable and interpretable association with damage outcomes in our analysis.

Regarding other variables, population density negatively correlates with affected farming/fishing households, and positively correlates with buildings flooded above floor (50-99 cm). Similar patterns of positive correlations were observed for total area and total population with flooding above floor (50-99 cm), partially destroyed buildings and affected employees. Larger populations and higher densities tend to occur in urban and developed areas (Marshall, 2007), which are less associated with farmlands. However, given Japan's geography, regions with a larger total population may also include farmland, increasing the likelihood of agricultural impacts. Higher income is likely associated with fewer flooded buildings because wealthier people tend to live in housing with better structure and protection (Phillips et al., 2005). Moreover, the number of affected farming/fishing households has increased over time, whereas affected underfloor households has decreased. This trend may reflect relatively lower disaster preparedness in farming/fishing communities (Carstens et al., 2025; Salam et al., 2023), in contrast to the gradual improvements in housing infrastructure (Marto et al., 2018), which enhance protection against TCs.

While our results suggest that along-track error shows the strongest and most consistent association with building-related flood damages — relative to haversine position, intensity, and landfall time errors — this does not imply that along-track forecasts are inherently more important. A more plausible interpretation is that improvements in some forecast components, particularly intensity, are harder to translate into actionable preparedness because of greater uncertainty, limited spatial specificity, and the difficulty of linking wind-based metrics to localized flood impacts. In contrast, along-track displacement directly affects which communities expect landfall, evacuation orders, and flood countermeasures, making improvements more immediately usable for decision-making. Therefore, the prominence of along-track error in our results likely reflects both its physical relevance and the current structure of disaster preparedness and communication systems, which more readily leverage track-related information than intensity or landfall timing forecasts.

In future work, a larger dataset would strengthen the robustness of the findings, as this study was limited to 31 landfalling TCs. Nevertheless, the results constitute a state-of-the-art dataset linking aggregated TC forecast errors with multiple damage indicators in Japan. Expanding the dataset and applying similar analyses to other regions would improve both accuracy and generalizability. It is also important to acknowledge that the relationship between forecast errors and damages is context-dependent. The damage-reduction benefit of improved forecasts does not manifest uniformly across events. Even highly accurate forecasts may yield limited societal benefit when risk communication is ineffective, compliance with protective actions is low, or warnings are issued too late to influence residents' behavior (Lindell & Perry, 2012; Morss et al., 2011). Additionally, insurance penetration, relief systems, previous disaster experience, social vulnerability, and local governance all mediate how forecast information is translated into damage reduction (Cutter et al., 2012; Raschky, 2008). Our analysis focuses on statistical associations between forecast errors and observed impacts, which reflect not only meteorological performance but also social, institutional, and behavioral factors. Future research should therefore integrate these contextual variables — such as warning dissemination quality, population responsiveness, and disaster education — into predictive frameworks. In particular, understanding whether individuals and decision-makers comprehend forecast content and associated probabilities is crucial, as actionable preparedness depends on more than forecast skill alone. Incorporating educational factors into predictive models could provide insights into potential behavioral responses, as knowledge is a fundamental component of disaster preparedness (Chen & Tseng, 2012; Hoffmann & Muttarak, 2017).

5 Data availability statement

TC best track positions and intensities from the Western Pacific can be obtained from JTWC (https://www.metoc.navy.mil/jtwc/jtwc.html?western-pacific), and JTWC forecasts from RAMMB (https://rammb-data.cira.colostate.edu/tc_realtime/). Statistics on damage and loss can be accessed on e-Stat (https://www.e-stat.go.jp/) and the Digital Typhoon dataset (https://agora.ex.nii.ac.jp). Statistical analyses were conducted using Python and spreadsheet software.

6 Acknowledgments

This project was supported by JST Moonshot R&D project (Grant no. JMPJMS2281), and JSPS Grant-in-Aid for Early-Career Scientists (Grant no. 23K13531). The authors declare no conflict of interest.

References

Barrett, B. S., Leslie, L. M., & Fiedler, B. H. (2006). An example of the value of strong climatological signals in tropical cyclone track forecasting: Hurricane ivan (2004). *Monthly weather review*, *134*(5), 1568–1577.

Cangialosi, J. P., Blake, E., DeMaria, M., Penny, A., Latto, A., Rappaport, E., & Tallapragada, V. (2020). Recent progress in tropical cyclone intensity forecasting at the national hurricane center. *Weather and Forecasting*, *35*(5), 1913–1922.

Carstens, J. D., Uejio, C. K., Powell, E., Jung, J., & Zonka, S. (2025). Tropical cyclones and climate change: An overview for the public health community. *Environmental Research*, 122149.

Chen, H.-R., & Tseng, H.-F. (2012). Factors that influence acceptance of web-based e-learning systems for the in-service education of junior high school teachers in taiwan. *Evaluation and program planning*, *35*(3), 398–406.

Conroy, A., Titley, H., Rivett, R., Feng, X., Methven, J., Hodges, K., Brammer, A., Burton, A., Chakraborty, P., Chen, G., et al. (2023). Track forecast: Operational capability and new techniques-summary from the tenth international workshop on tropical cyclones (iwtc-10). *Tropical Cyclone Research and Review*, *12*(1), 64–80.

Cutter, S. L., Boruff, B. J., & Shirley, W. L. (2012). Social vulnerability to environmental hazards. In *Hazards vulnerability and environmental justice* (pp. 115–132). Routledge.

Digital Typhoon. (2025a). Digital typhoon: Typhoon damage list [Accessed: 2025-05-02].

Digital Typhoon. (2025b). Digital typhoon: Typhoon landfall and passage database (full version) [Accessed: 2025-05-02].

Dilley, M. (2005). *Natural disaster hotspots: A global risk analysis* (Vol. 5). World Bank Publications.

e-Stat. (2025). Flood damage statistics survey / 2020 flood damage statistics survey / basic flood damage statistics table (suigai tōkei chōsa/ ryō wa 2-nen suigai tōkei chōsa/ suigai tōkei kihon-hyō) [Accessed: 2025-06-26].

Hanson, S., Nicholls, R., Ranger, N., Hallegatte, S., Corfee-Morlot, J., Herweijer, C., & Chateau, J. (2011). A global ranking of port cities with high exposure to climate extremes. *Climatic change*, *104*(1), 89–111.

Hoffmann, R., & Muttarak, R. (2017). Learn from the past, prepare for the future: Impacts of education and experience on disaster preparedness in the philippines and thailand. *World Development*, *96*, 32–51.

Huang, X., Peng, X., Fei, J., Cheng, X., Ding, J., & Yu, D. (2021). Evaluation and error analysis of official tropical cyclone intensity forecasts during 2005–2018 for the western north pacific. *Journal of the Meteorological Society of Japan. Ser. II*, *99*(1), 139–163.

Islam, M. R., & Sawada, Y. (2025). Multi-dimensional risk ranking of historical tropical cyclones. *Bulletin of the American Meteorological Society*, BAMS–D.

Ito, K. (2016). Errors in tropical cyclone intensity forecast by rsmc tokyo and statistical correction using environmental parameters. *Sola*, *12*, 247–252.

Joint Typhoon Warning Center, J. T. W. C. (2025). Best track data [Accessed: 2025-05-02].

Kato, F., & Tajima, Y. (2023). Coastal adaptation to climate change in japan: A review. *Coastal Engineering Journal*, *65*(4), 597–619.

Kaźmierczak, A., & Cavan, G. (2011). Surface water flooding risk to urban communities: Analysis of vulnerability, hazard and exposure. *Landscape and urban planning*, *103*(2), 185–197.

Knapp, K. R., Kruk, M. C., Levinson, D. H., Diamond, H. J., & Neumann, C. J. (2010). The international best track archive for climate stewardship (ibtracs) unifying tropical cyclone data. *Bulletin of the American Meteorological Society*, *91*(3), 363–376.

LeComte, D. (2020). International weather events 2019: Historic heat, hurricanes, and fires. *Weatherwise*, *73*(3), 24–31.

Leonardo, N. M., & Colle, B. A. (2020). An investigation of large along-track errors in extratropical transitioning north atlantic tropical cyclones in the ecmwf ensemble. *Monthly Weather Review*, *148*(1), 457–476.

Leroux, M.-D., Wood, K., Elsberry, R. L., Cayanan, E. O., Hendricks, E., Kucas, M., Otto, P., Rogers, R., Sampson, B., & Yu, Z. (2018). Recent advances in research and forecasting of tropical cyclone track, intensity, and structure at landfall. *Tropical Cyclone Research and Review*, *7*(2), 85–105.

Lindell, M. K., & Perry, R. W. (2012). The protective action decision model: Theoretical modifications and additional evidence. *Risk Analysis: An International Journal*, *32*(4), 616–632.

Marshall, J. D. (2007). Urban land area and population growth: A new scaling relationship for metropolitan expansion. *Urban studies*, *44*(10), 1889–1904.

Martinez, A. B. (2020). Forecast accuracy matters for hurricane damage. *Econometrics*, *8*(2), 18.

Marto, R., Papageorgiou, C., & Klyuev, V. (2018). Building resilience to natural disasters: An application to small developing states. *Journal of Development Economics*, *135*, 574–586.

McAdie, C. J., & Lawrence, M. B. (2000). Improvements in tropical cyclone track forecasting in the atlantic basin, 1970–98. *Bulletin of the American Meteorological Society*, *81*(5), 989–998.

Meiler, S., Vogt, T., Bloemendaal, N., Ciullo, A., Lee, C.-Y., Camargo, S. J., Emanuel, K., & Bresch, D. N. (2022). Intercomparison of regional loss estimates from global synthetic tropical cyclone models. *Nature Communications*, *13*(1), 6156.

Minamide, M., & Posselt, D. J. (2025). Improving tropical cyclone intensification prediction using high-resolution all-sky geostationary operational environmental satellite data assimilation. *Quarterly Journal of the Royal Meteorological Society*, e4958.

Morss, R. E., Lazo, J. K., & Demuth, J. L. (2010). Examining the use of weather forecasts in decision scenarios: Results from a us survey with implications for uncertainty communication. *Meteorological Applications*, *17*(2), 149–162.

Morss, R. E., Wilhelmi, O. V., Meehl, G. A., & Dilling, L. (2011). Improving societal outcomes of extreme weather in a changing climate: An integrated perspective. *Annual Review of Environment and Resources*, *36*(1), 1–25.

Peduzzi, P., Chatenoux, B., Dao, H., De Bono, A., Herold, C., Kossin, J., Mouton, F., & Nordbeck, O. (2012). Global trends in tropical cyclone risk. *Nature climate change*, *2*(4), 289–294.

Phillips, B. D., Metz, W. C., & Nieves, L. A. (2005). Disaster threat: Preparedness and potential response of the lowest income quartile. *Global Environmental Change Part B: Environmental Hazards*, *6*(3), 123–133.

Powell, M. D., & Aberson, S. D. (2001). Accuracy of united states tropical cyclone landfall forecasts in the atlantic basin (1976–2000). *Bulletin of the American Meteorological Society*, *82*(12), 2749–2768.

Raschky, P. A. (2008). Institutions and the losses from natural disasters. *Natural hazards and earth system sciences*, *8*(4), 627–634.

Regional & Mesoscale Meteorology Branch, R. A. M. M. B. (2025). Tropical cyclone archive [Accessed: 2025-05-02].

Ren, F., Wang, Y., Wang, X., & Li, W. (2007). Estimating tropical cyclone precipitation from station observations. *Advances in atmospheric sciences*, *24*(4), 700–711.

Roy, C., & Kovordányi, R. (2012). Tropical cyclone track forecasting techniques–a review. *Atmospheric research*, *104*, 40–69.

Salam, A., Wireko, A. A., Jiffry, R., Ng, J. C., Patel, H., Zahid, M. J., Mehta, A., Huang, H., Abdul-Rahman, T., & Isik, A. (2023). The impact of natural disasters on healthcare and surgical

services in low-and middle-income countries. *Annals of Medicine and Surgery*, *85*(8), 3774–3777.

Salomon, E. (2024). The value of improving hurricane forecasts [Accessed: 2025-09-16].

Sampson, C. R., & Schrader, A. J. (2000). The automated tropical cyclone forecasting system (version 3.2). *Bulletin of the American Meteorological Society*, *81*(6), 1231–1240.

Sawada, Y., Yagi, R., Kawabata, T., & Kotani, H. (2025). *Cry wolf effect in flood early warning* [Unpublished manuscript (in review)].

Shi, R., & Xu, F. (2024). Improvement of global forecast of tropical cyclone intensity by spray heat flux and surface roughness. *Journal of Geophysical Research: Atmospheres*, *129*(8), e2023JD039624.

Shimozono, T., Tajima, Y., Kumagai, K., Arikawa, T., Oda, Y., Shigihara, Y., Mori, N., & Suzuki, T. (2020). Coastal impacts of super typhoon hagibis on greater tokyo and shizuoka areas, japan. *Coastal Engineering Journal*, *62*(2), 129–145.

Takagi, H., Anh, L. T., Islam, R., & Hossain, T. T. (2023). Progress of disaster mitigation against tropical cyclones and storm surges: A comparative study of bangladesh, vietnam, and japan. *Coastal Engineering Journal*, *65*(1), 39–53.

Wirtz, A., Kron, W., Löw, P., & Steuer, M. (2014). The need for data: Natural disasters and the challenges of database management. *Natural Hazards*, *70*(1), 135–157.

World Meteorological Organization, W. M. O. (2020). Tropical cyclone [Accessed: 2025-05-02].